MODELING A MORBILLIVIRUS OUTBREAK IN HAWAIIAN MONK SEALS TO AID IN THE DESIGN OF MITIGATION PROGRAMS

Jason D. Baker,[1,4] **Albert L. Harting,**[2] **Michelle M. Barbieri,**[1] **Stacie J. Robinson,**[1] **Frances M.D. Gulland,**[3] **and Charles L. Littnan**[1]

[1] Pacific Islands Fisheries Science Center, National Marine Fisheries Service, National Oceanic and Atmospheric Administration 1845 Wasp Blvd. No. 176, Honolulu, Hawaii, 96818 USA
[2] Harting Biological Consulting, 8898 Sandy Creek Lane, Bozeman, Montana 59715, USA
[3] The Marine Mammal Center, Sausalito, California 94965, USA
[4] Corresponding author (email: jason.baker@noaa.gov)

ABSTRACT: We developed a stochastic susceptible–exposed–infectious–removed (SEIR) model to simulate a range of plausible morbillivirus outbreak scenarios in a randomly mixing population of 170 endangered Hawaiian monk seals (*Neomonachus schauinslandi*). We then modeled realistic vaccination and quarantine measures to determine the potential efficacy of such mitigation efforts. Morbillivirus outbreaks represent substantial risk to monk seals—91% of simulated baseline outbreaks grew ($R_0>1$), and in one-third of the scenarios all, or nearly all, individuals were infected. Simulated vaccination efforts in response to an outbreak were not effective in substantially reducing infections, largely because of the prolonged interval between vaccination and immunity. Prophylactic vaccination, in contrast, could be an effective tool for preventing outbreaks. Herd immunity is practically achievable because of the small sizes of monk seal populations and the animals' accessibility on shore. Adding realistic spatial structure to the model, as informed by movement of seals tracked in the main Hawaiian Islands with the use of telemetry, greatly reduced the simulated impact of outbreaks (≤10 seals were infected in 62% of spatially structured simulations). Although response vaccination remained relatively ineffective, spatial segregation allowed herd immunity to be achieved through prophylactic vaccination with less effort. In a randomly mixing population of 170 seals, 86% would need to be vaccinated to achieve herd immunity in 95% of simulated outbreaks, compared to only approximately 60% in three spatially segregated subgroups with the same combined abundance. Simulations indicate that quarantining a modest number (up to 20) of ill seals has the potential to extinguish even fast-growing outbreaks rapidly. The efficacy of quarantine, however, is highly dependent upon rapid detection and response. We conclude that prophylactic vaccination combined with a quarantine program supported by vigilant surveillance and rapid, reliable diagnosis could greatly mitigate the threat of a morbillivirus outbreak in Hawaiian monk seals.

Key words: Hawaiian monk seal, morbillivirus, SEIR model, quarantine, vaccination.

INTRODUCTION

Epizootic disease can have devastating effects on wildlife populations, especially on isolated or small populations (MacPhee and Greenwood 2013; Gordon et al. 2015). Approximately 1,300 Hawaiian monk seals (*Neomonachus schauinslandi*) remain throughout the Hawaiian Archipelago (Baker et al. 2016b). The species has extremely low genetic diversity (Schultz et al. 2009) and has not been exposed to many mammalian diseases because of its isolation for millions of years (Scheel et al. 2014). Consequently, outbreaks of diseases to which monk seals have not been previously exposed could have devastating impacts. Morbilliviruses, specifically phocine distemper virus (PDV) and canine distemper virus (CDV),

have caused mass die-offs of phocids (Grachev et al. 1989; Heide-Jørgensen and Harkonen 1992; Kennedy et al. 2000; Jensen et al. 2002). To date, surveys for infectious disease indicate that Hawaiian monk seals have not been exposed to morbilliviruses (Aguirre et al. 2007). Thus, their naivety to morbillivirus exposure increases concern about potential impacts of an epizootic in monk seals.

Infectious disease modeling can elucidate the likely course of outbreaks and help identify the most effective and efficient approaches to their mitigation (Vynnycky and White 2010). Available tools to prevent or control disease outbreaks in wild populations include vaccination (either prophylactic or in response to an outbreak), quarantine, and culling. Because of the endangered status

of Hawaiian monk seals, culling is not considered a viable option.

Here, we present a modeling effort that integrates relevant information about morbilliviruses in general, PDV in phocids in particular, and species-specific information on Hawaiian monk seal population dynamics, spatial structure, and contact patterns. The model is used both to simulate a range of plausible outbreak trajectories and to explore mitigation options. Because there are great uncertainties associated with many of the model parameters, we do not attempt to predict the most likely outcomes. Rather, our objective is to identify which measures, applied at practically achievable scales, have the potential to prevent or minimize the growth of a simulated plausible range of morbillivirus outbreak trajectories.

MATERIALS AND METHODS

Baseline susceptible–exposed–infectious–removed model

To generate a baseline range of plausible outbreaks, we used a simple compartmental susceptible–exposed–infectious–removed (SEIR) model (Vynnycky and White 2010). In the model, the epidemic is initiated by the introduction of an exposed individual into the population, and the model then tracks the progression of the outbreak as individual seals transition among states (susceptible, exposed, etc.). We assume that any morbillivirus infection and the vaccine will be permanently immunizing (Duignan et al. 2014). Although we cannot predict the lethality of a morbillivirus infection in monk seals, the final model compartment (removed) accommodates both survivors with life-long immunity and fatalities, which are equivalent in terms of modeling. The simulated population is closed (does not change due to births, deaths, immigration, or emigration).

The SEIR model is governed by the following equations:

$$S_{t+1} = S_t - -\beta(S_t I_t)$$

$$E_{t+1} = E_t + \beta(S_t I_t) - \sigma E_t$$

$$I_{t+1} = I_t + \sigma E - \gamma I_t$$

$$R_{t+1} = R_t + \gamma I_t$$

where S_t, E_t, I_t, and R_t are the number of susceptible, exposed, infectious, and removed individuals at time t (in days). Their sum is N, the total population size. The effective contact rate (β) is the probability of effective contact between two specific individuals per day, and we assume random mixing among individuals. As is common for wildlife populations, we assume contact is density dependent (Vynnycky and White 2010). The rate at which exposed individuals become infectious (σ) is the inverse of the latency period, and γ is the rate at which infectious individuals recover or die (inverse of the infectious period, D).

Ours is a discrete time model, with each time step equal to 1 d, such that all temporal rate parameters are defined per day. Each day, the value for the number of individuals in each compartment is equal to the number present at the previous day adjusted in accordance with the incremental change described by the preceding difference equations (Fig. 1A).

Vaccination response module

We expanded the baseline SEIR model to simulate a program of post-outbreak vaccination response. The following additional parameters governed the progression of this module: 1) n_{det} is the threshold number of infectious seals for an outbreak to be detected, 2) t_{resp} is the time for managers to mount a response and begin vaccination, 3) v is the vaccination rate (proportion of susceptible and exposed seals vaccinated per day), and 4) t_{imm} is the number days from vaccination until immunity.

In a simulated response vaccination scenario, an outbreak begins according to the baseline scenario, and once n_{det} seals have become infectious, the outbreak is detected. Following t_{resp} days of mobilization, vaccination of any seals that have not already exhibited symptoms (susceptible and exposed) are vaccinated at a constant rate (v). Any seal that has already been exposed, or becomes exposed within t_{imm} days of being vaccinated, will become infectious. Those that are not exposed prior to, or within t_{imm} days postvaccination, become immune and move to the removed compartment (Fig. 1B).

Prophylactic vaccination and herd immunity

Use of prophylactic vaccination to confer herd immunity prior to an outbreak is a further mitigation measure. Herd immunity is achieved when sufficient individuals are immunized such that the number of susceptible seals in the population is reduced to a level whereby $R_0 < 1$ (Vynnycky and White 2010, defined above as the product βND). Substituting 1 for R_0 and S for N
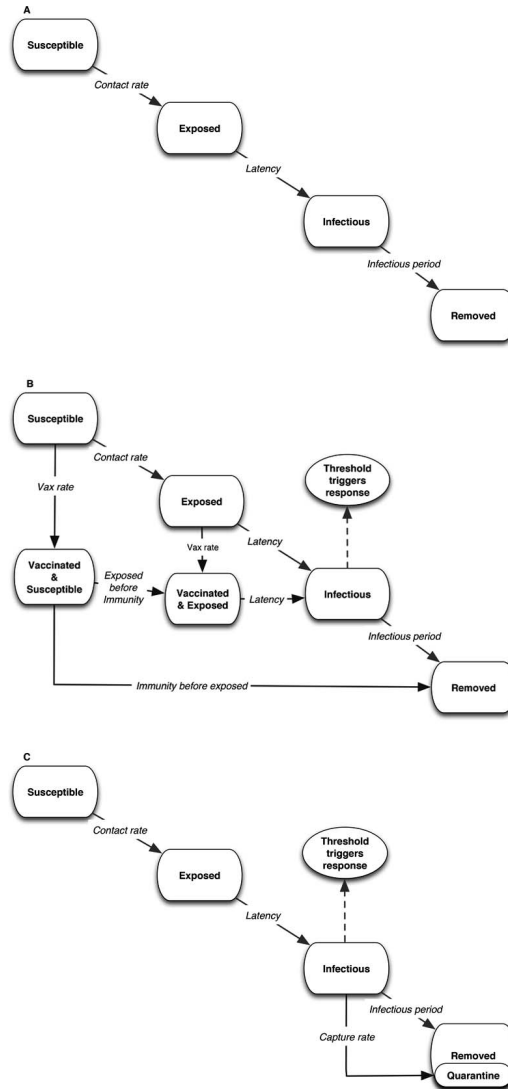
FIGURE 1. (A) The baseline Hawaiian monk seal (*Neomonachus schauinslandi*) susceptible–exposed–infectious–recovered (SEIR) simulation model process. At the start of a simulation, an exposed individual is introduced into an entirely susceptible population and becomes infectious following the latent period. Susceptible individuals become exposed through effective contact with infectious individuals (according to the contact rate). Exposed individuals become infectious after latency, and finally move to the removed compartment following the infectious period. (B) The Hawaiian monk seal (*Neomonachus schauinslandi*) SEIR model with response vaccination module is identical to the baseline, except that after a threshold number of infectious individuals exists, the outbreak is detected. Next, after the response time elapses, vaccination of apparently healthy individuals (susceptible and exposed) is carried out according to the vaccination rate. Vaccination of exposed individuals has no effect; they become infectious following latency. Susceptible individuals that are vaccinated may become exposed (to infectious individuals according to the contact rate) before the time to immunity has elapsed, and then progress to infectious and removed. Alternatively, if susceptible vaccinated individuals are not exposed before the time to immunity has elapsed, they become immune, and move to the removed compartment, bypassing the infectious compartment. (C) The Hawaiian monk seal (*Neomonachus schauinslandi*) SEIR model with quarantine response module is identical to the baseline, except that after a threshold number of infectious individuals exists, the outbreak is detected. Next, after the response time elapses, ill (infectious) individuals are captured according to the quarantine rate and moved directly to the removed compartment.

and rearranging gives the maximum number of susceptible individuals that may exist and achieve herd immunity: $(\beta D)^{-1}$. In a fully unexposed and unvaccinated population, all individuals are susceptible such that initially, S is equivalent to the total population size (N). Thus, $N-(\beta D)^{-1}$ represents the number of individuals that must be vaccinated to achieve herd immunity in a total population of N. We used the random combinations of β and D from the baseline scenarios along with a fixed N (170 seals) to generate a distribution of the number of seals to vaccinate for herd immunity.

Quarantine module

This module simulates quarantine of ill individuals, thereby removing them from the infectious compartment. Parameters involved in simulating quarantine include: n_{det} and t_{resp} defined as above, and q is the capture rate (proportion of infectious seals brought into quarantine per day), and q_{max} is the maximum number of individuals that can be held in quarantine.

Under this scenario, once an outbreak occurs, is detected (per n_{det}) and quarantine is initiated (per t_{resp}), recognizably ill seals (infectious) are captured and brought into quarantine according to q, until the capacity for quarantine (q_{max}) has been met, at which time no additional seals are brought into quarantine. Quarantined seals are treated as removed (Fig. 1C).

Parameter distributions and simulation process

Considerable uncertainty is associated with all of the key parameters that drive the baseline SEIR model, as well as the vaccination and quarantine modules. The best estimates for each parameter and their associated ranges were derived from information about Hawaiian monk seal biology, decades of experience with fieldwork logistics, PDV outbreak parameters, and vaccination trials in other seal species. These values are presented in the Results and their supporting information is documented in the Supplementary Material. We generated uniform distributions bounded by each parameter's plausible range. For most parameters, the range was not symmetrical around the best estimate. We therefore partitioned each parameter into a stepped uniform distribution where the median value equals the best estimate.

The Hawaiian monk seal (*Neomonachus schauinslandi*) metapopulation comprises multiple subpopulations distributed throughout the 2,600-km-wide Hawaiian Archipelago (Fig. 2). Most seals reside in the remote Northwestern Hawaiian Islands, and the remainder in the main Hawaiian Islands (Baker et al. 2011). Because of their remote nature and limited human presence, there is relatively low probability of timely detection and response to outbreaks in the Northwestern Hawaiian Islands. In contrast, seals are conspicuous and accessible in the main Hawaiian Islands; thus we designed the simulations to represent this latter region. For example, we specified a fixed population size of 170 seals for all simulations, which is comparable to recent estimates for the main Hawaiian Islands (Baker et al. 2011).

To generate a range of plausible baseline outbreak trajectories, 1,000 SEIR parameter sets were randomly drawn from the distributions for contact rate, latency, and infectious period. A 200-d outbreak was then simulated for each of the 1,000 parameter sets, and summary information, such as the basic reproductive number, R_0, and total number of seals infected, was stored. The expected number of secondary infections arising from an infectious individual entering an entirely susceptible population (R_0) is directly calculable, thus:

$$R_0 = bND$$

where, again, β is the contact rate, N is the total population size, and D is the duration of the infectious period, or the inverse of γ (Vynnycky and White 2010).

To evaluate vaccination response as a tool to mitigate outbreaks, 1,000 vaccination response trajectories (using parameter sets randomly drawn from the distributions of n_{det}, t_{resp}, v, and t_{imm}) were run for each of the above 1,000 baseline scenarios, and summary statistics such as mean, median, 5th and 95th percentiles of the resulting number of seals infected, were stored. Mean vaccination efficacy was calculated as the mean proportional reduction in infections with vaccination compared to baseline. Quarantine response efficacy was evaluated in an analogous manner, with 1,000 quarantine simulations for each of the 1,000 baseline scenarios.

Heterogeneous contact—size and sex class

The simulations described thus far assumed random (homogeneous) contact among all members of the population. However, Baker et al. (2016a) found statistically significant differences in contact rates within and among some size/age and sex classes of Hawaiian monk seals. We used a more complex model with heterogeneous contact to explore whether these class-specific contact rates would substantially influence outbreak trajectories.

We created a heterogeneous contact model with four size classes (pup, juvenile, subadult, and
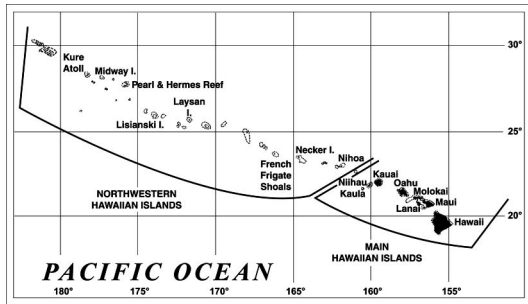
FIGURE 2.   The Hawaiian Archipelago, with demarcations showing the extent of the Northwestern and main Hawaiian Islands. Place names of most islands and atolls where Hawaiian monk seals (*Neomonachus schauinslandi*) occur are noted.

adult) and two sexes, for a total of eight classes, and 36 unique intra- and interclass pairings following Baker et al. (2016a). Contact rates between classes i and j are denoted by β_{ij}, and the heterogeneous contact model maintains separate accounting for the number of seals in each class within each SEIR category. Contact rates govern changes in the susceptible and exposed model compartments. At each time step, the number of susceptible seals in class i that become exposed is the sum of the number of susceptible seals of class i exposed to infectious seals of all classes, calculated using the unique β_{ij} for each inter-class pairing. Thus, the number of exposed seals in class i at time $t+1$ is

$$E_{i,t+1} = E_{i,t} + \sum_{j=1}^{8} \beta_{ij}(S_{i,t}I_{j,t}) - \sigma E_{i,t}$$

Similarly, the summation term above gives the reduction in number of susceptible seals in class i that transition from susceptible to exposed.

With the use of association data, Baker et al. (2016a) estimated a population mean β assuming random mixing, as well as 36 β_{ij}s for the monk seal population residing at Laysan Island in 1991. To evaluate the influence of homogeneous contact on outbreak trajectories, we compared a set of simulations using the baseline SEIR model with a fixed β assuming random mixing, to a separate set of simulations using the heterogeneous contact model parameterized with the β_{ij}s estimated by Baker et al. (2016a). Trajectories using all possible combinations for the remaining SEIR parameters (latency and infectious period) were run in both the homogeneous and heterogeneous contact models. Further, in the heterogeneous contact model, the class of the first exposed individual was randomly assigned in each simulation. Finally, recognizing that the size and sex class structure of the simulated population could influence the trajectory of outbreaks with heterogeneous con-

tact, we conducted the above comparison of homogeneous with heterogeneous contact using two different realistic class structures. The first was that observed at Laysan Island 1991 (the population in which the contact rates were estimated), and other was the estimated size/sex structure of the population in the main Hawaiian Islands in 2014 (Table 1; Johanos 2015a, b). Both structures were scaled to total population size of 170 seals.

Influence of spatial structure

Spatial structuring of the population could also influence contact patterns and outbreak trajectories, as seals present on the same island will have a higher probability of contacting one another than a seal on a different island. To explore this matter, we constructed a spatially structured model featuring separate spatial nodes in each of which

TABLE 1.   Hawaiian monk seal (*Neomonachus schauinslandi*) body size and sex class structures at Laysan Island in 1991, and in the main Hawaiian Islands in 2014. Values indicate the proportion of the total population in each class.

	Proportion of the total population	
Class	Laysan Island (1991)	Main Hawaiian Islands (2014)
Adult female	0.294	0.224
Adult male	0.353	0.241
Subadult female	0.047	0.071
Subadult male	0.053	0.082
Juvenile female	0.053	0.094
Juvenile male	0.076	0.082
Pup female	0.041	0.076
Pup male	0.082	0.129

ran an SEIR model (identical to that depicted in Fig. 1A). All individual seals within each node were subject to daily probabilities of moving between nodes. Outbreaks were initiated by introducing a single exposed seal to one of the nodes (randomly selected). Outbreaks then grew within the initial node and would spread to other node(s) if one or more exposed or infectious seals moved. In order to maintain comparability with the baseline SEIR (nonspatially structured) simulations, the total population of individual seals was equally divided among spatial nodes at the initiation of each simulation. As above, 1,000 simulations with randomly drawn parameters were performed, each one now combined with random movement realizations. Finally, to evaluate how the efficacy of response vaccination might be affected by seal movement patterns, we also conducted vaccination response simulations (as in Fig. 1B) incorporating spatial structure as above. In these scenarios, once an outbreak has been detected, vaccination is initiated at all spatial nodes simultaneously.

The number of nodes and movement rates amongst nodes was determined with the use of data from 20 monk seals tracked with global positioning system (GPS) cell phone instruments in the main Hawaiian Islands during 2007–2014 (Wilson 2015; Robinson 2016). Daily movement rates were estimated with the use of the number of documented movements between two specific islands completed by all seals divided by the total number of seal tracking days.

Summary of simulation scenarios and comparisons

We compared the above series of simulation scenarios to elucidate both patterns that influenced the plausible range of outbreak trajectories, as well as which mitigation measures, vaccination or quarantine, might prove effective in mitigating outbreaks. Table 2 summarizes the specific comparisons made and the insights they were designed to provide.

RESULTS

Parameter space

Best estimates and ranges for parameters governing transition among baseline SEIR model compartments as well as parameters governing vaccination and quarantine response are presented in Table 3. For details regarding how these values were determined see Supplementary Materials.

Baseline simulations

The behavior of the simulated baseline outbreaks was variable and exhibited realistic properties and trajectories. For example, the distribution of R_0 values had a wide range but presented a strong mode between 1 and 2.5, which corresponds with the range of R_0 values Lonergan et al. (2010) estimated for the 1988 and 2002 PDV outbreaks in UK harbor seals (Fig. 3). The basic reproductive number (R_0) exceeded 1 in 91% of the baseline scenarios, meaning that in these cases the outbreak would grow. In 33% of the scenarios, all or nearly all (≥ 167) of the 170 seals became infected by day 200. The median number infected was 156.

Vaccination

We compared the total number of seals infected in simulations with and without vaccination response, but only for those baseline scenarios where $R_0 \geq 1$ (thereby excluding trivial cases where the simulated outbreak would not grow). The mean response vaccination efficacy was only 0.15. Expected efficacy peaked at 0.42 in scenarios where R_0 was approximately 1.6 and rapidly declined at higher values (Fig. 4). The limited efficacy was not due to failure to administer vaccinations; the simulated mean number vaccinated in all scenarios with $R_0 > 1$ was 113 seals in a total population of 170. Rather, a large portion of the seals vaccinated had either already been exposed (especially in faster growing outbreaks) or became exposed after vaccination but prior to achieving immunity. In contrast, analysis of the baseline scenarios revealed that to achieve herd immunity in 95% of the simulated baseline outbreaks, 86% (146 seals) of the population would need to be prophylactically vaccinated.

Heterogeneous contact

Comparison of scenarios with random versus heterogeneous contact revealed that the observed class-specific contact patterns (Baker et al. 2016a) had little influence on outbreak trajectories. The total number of

TABLE 2. Summary of susceptible–exposed–infectious–recovered (SEIR) model scenarios used to address specific questions regarding plausible trajectories of morbillivirus outbreaks in simulated Hawaiian monk seal (*Neomonachus schauinslandi*) populations. The potential efficacies of mitigation measures (response vaccination and quarantine) are also assessed.

Scenarios compared	Question
Baseline versus vaccination response	Is response vaccination likely to reduce the number of seals infected substantially?
Baseline versus class-specific contact	Is heterogeneous contact among size and sex classes likely to influence outbreak trajectories substantially?
Baseline versus spatially structured	Are observed spatial structure and movement patterns of seals in the main Hawaiian Islands likely to influence outbreak trajectories substantially?
Spatially structured no response versus spatially structured vaccination response	Are observed spatial structure and movement patterns of seals in the main Hawaiian Islands likely to influence the efficacy of response vaccination?
Baseline versus quarantine response	Is quarantine response likely to reduce the number of seals infected substantially?

seals infected did not vary appreciably either with homogeneous or heterogeneous mixing, regardless of which size-sex class structure was simulated or which class of seal was first exposed (Fig. 5).

Spatial structure

Twenty seals fitted with GPS tags were tracked for a combined total of 2,988 seal-days. Seven seals were tagged on Kauai, seven on Oahu, and six on Molokai, and at least one of these seals was documented at all eight main Hawaiian Islands. To simplify the spatially structured SEIR model, we partitioned the main Hawaiian Islands into three nodes. There was frequent movement between adjacent Ni'ihau and Kauai Islands, so these were combined as one node. Oahu was a second node, and the four nearby islands that constitute Maui Nui (Molokai, Lanai, Kahoolawe, and Maui) were combined as the third node. There was only one documented movement to Hawaii Island at the eastern end of the archipelago, and very few monk seals use that island, so it was excluded from spatial analysis.

TABLE 3. Parameter space for susceptible–exposed–infectious–recovered (SEIR) modeling of morbillivirus outbreaks in Hawaiian monk seals (*Neomonachus schauinslandi*). Lowest and highest values define the range, with best values also provided. See Supplementary Materials for further detail.

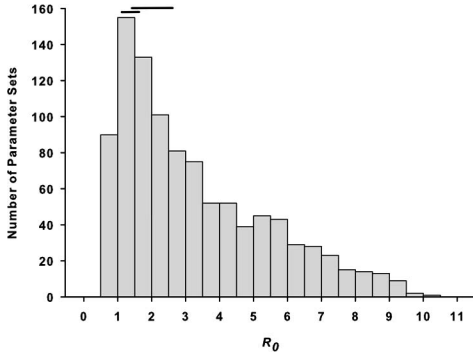|	Values		
Parameter	Lowest	Best	Highest
Contact rate (β)	0.000374	0.001122	0.003366
Latency period ($1/\sigma$)	1 d	5 d	7 d
Infectious period ($D=1/\gamma$)	7 d	12 d	18 d
Threshold ill seals to detect outbreak (N_{det})	1	10	30
Response time (t_{resp})	0 d	2 d	4 d
Vaccination rate (v)	0.01	0.07	0.20
Time to immunity (t_{imm})	21	45	120
Quarantine capture rate (q)		0.5	
Maximum in quarantine (q_{max})		20	

FIGURE 3. Distribution of 1000 R_0 values from baseline morbillivirus outbreak simulations in a Hawaiian monk seal (*Neomonachus schauinslandi*) population. The solid line above the distribution indicates the 95% confidence interval ranges estimated for 1988 (lower line) and 2002 (upper line) phocine distemper virus (PDV) outbreaks in UK harbor seals (*Phoca vitulina*, from Lonergan et al. 2010).

No seal was documented moving directly between Maui Nui and Kauai-Ni'ihau without landing at Oahu on the way. Therefore, the spatial SEIR model incorporated two bidirectional daily per capita movement rates linking the three nodes: Kauai-Ni'ihau to/from Oahu at 0.0031 movements/(seal×day) and Oahu to/
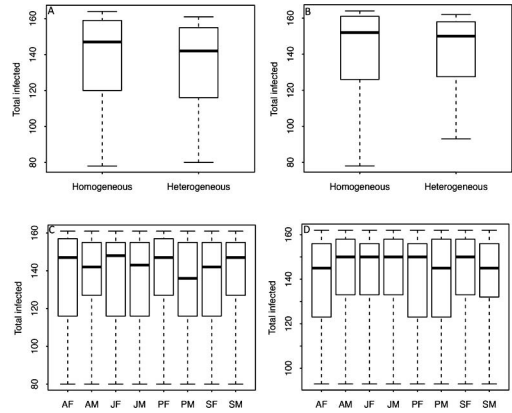

FIGURE 5. Distributions of the total number of Hawaiian monk seals (*Neomonachus schauinslandi*) infected during 1,000 simulated morbillivirus outbreaks. Box plots indicate median (dark line), 25th and 75th percentiles (box), and range (whiskers). (A) Homogeneous and heterogeneous contact with Laysan Island 1991 size and sex class structure. (B) Homogeneous and heterogeneous contact with main Hawaiian Islands 2014 size and sex class structure. (C) Heterogeneous contact showing variation with size and sex of the first individual exposed, Laysan Island 1991 age and sex structure. (D) Heterogeneous contact showing variation with size and sex of the first individual exposed, main Hawaiian Islands 2014 age and sex structure. A=adult, S=subadult, J=juvenile, P=pup, F=female, M=male.

from Maui Nui at 0.0048 movements/(seal×day).

Introducing spatial structure in the modeled population strongly affected the outcome of simulated outbreaks. The distribution of the total number of seals infected in the spatially structured scenarios was markedly different from the baseline scenarios (Fig. 6). Fewer than 10 seals were infected in 62% of the spatially structured scenarios.

Although the simulated growth and extent of outbreaks was greatly reduced when spatial structure was incorporated into the model, the mean efficacy of response vaccination was only slightly higher (0.18 versus 0.15) than in the baseline scenario. In contrast, the existence of three semi-isolated spatial nodes within the modeled population effectively reduced the threshold for achieving herd immunity through prophylactic vaccination. If the three separate nodes were completely isolated, their combined abundance was N,

FIGURE 4. Relationship between efficacy of response vaccination, defined as the proportional reduction in infections, and R_0, the basic reproductive number in morbillivirus outbreak simulations in a Hawaiian monk seal (*Neomonachus schauinslandi*) population. For each of 1,000 baseline outbreak simulations, 1,000 vaccination response scenarios were run. Mean (open circles), fifth (filled circles), and 95th percentiles (crosses) represent the distribution of response vaccination efficacy for each baseline scenario.
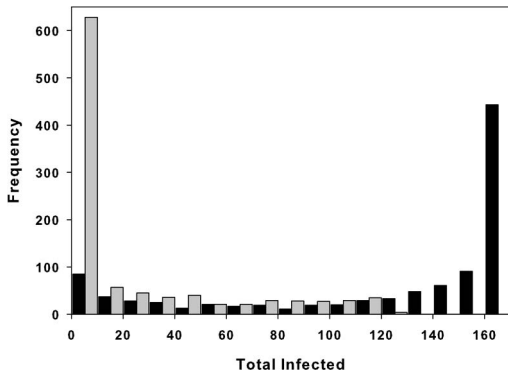
FIGURE 6.   Distributions of the number of Hawaiian monk seals (*Neomonachus schauinslandi*) seals infected during simulated morbillivirus outbreaks in a total population of 170. Black bars represent 1,000 baseline scenarios in which the entire population is randomly mixing. Grey bars represent 1,000 spatially structured scenarios in which the population is divided into three separate nodes. Seals mix randomly within each node and move between nodes according to daily probabilities.

FIGURE 7.   Relationship between efficacy of quarantine, defined as the proportional reduction in infections, and R_0, the basic reproductive number in morbillivirus outbreak simulations in a Hawaiian monk seal (*Neomonachus schauinslandi*) population. For each of 1,000 baseline outbreak simulations, 1,000 quarantine scenarios were run. Mean (open circles), fifth (filled circles), and 95th percentiles (crosses) represent the distribution of quarantine efficacy for each baseline scenario.

and at least $(\beta D)^{-1}$ individuals were present in each node, then the number required to vaccinate in order to achieve herd immunity in all three nodes would be $N–3(\beta D)^{-1}$, which is less than required in a single population of size N, namely, $N–(\beta D)^{-1}$. This is approximately the same situation as the spatially structured model scenario, except that the modeled nodes are linked by small daily movement probabilities, such that chance movements could marginally diminish herd immunity. Applying the calculation above for three segregated nodes shows that herd immunity could be achieved in approximately 95% of the spatially structured scenarios by prophylactically vaccinating 60% of the seals within each node (compared to 86% in the baseline scenarios).

Quarantine

Efficacy of quarantining ill animals in response to an outbreak varied greatly with R_0, but also strongly depended upon how rapidly quarantine began. When R_0 was low (just above one), mean efficacy was also low but rapidly rose to a peak of nearly 90% reduction in infections when $R_0 \approx 2$ (Fig. 7). As
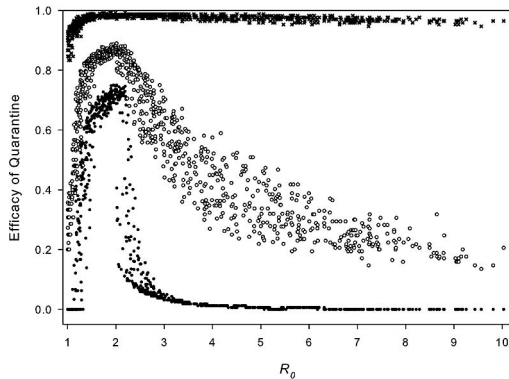
R_0 increased beyond 2, mean efficacy steadily declined, accompanied by a dramatic increase in the range of outcomes, such that the fifth and 95th percentiles were approximately 0 and 1, respectively. This variability in efficacy was largely driven by the threshold for detecting an outbreak (n_{det}) and the time between detection and commencing quarantine (t_{resp}). For example, if the first ill animal were detected ($n_{det}=1$), outbreaks could be effectively halted even if initiation of quarantine was delayed up to 4 d, regardless of the R_0 value (Fig. 8A). Even if six animals were ill prior to detection ($n_{det}=6$), quarantine could still limit the number of infections, especially if response time were rapid (Fig. 8B). However, at higher values of n_{det}, infections would tend outrun the quarantine effort, resulting in limited efficacy, especially at higher R_0 values (Fig. 8C–F).

DISCUSSION

The baseline SEIR scenarios were intended to provide a plausible range of morbillivirus outbreak scenarios against which to measure the relative efficacy of mitigation actions. This
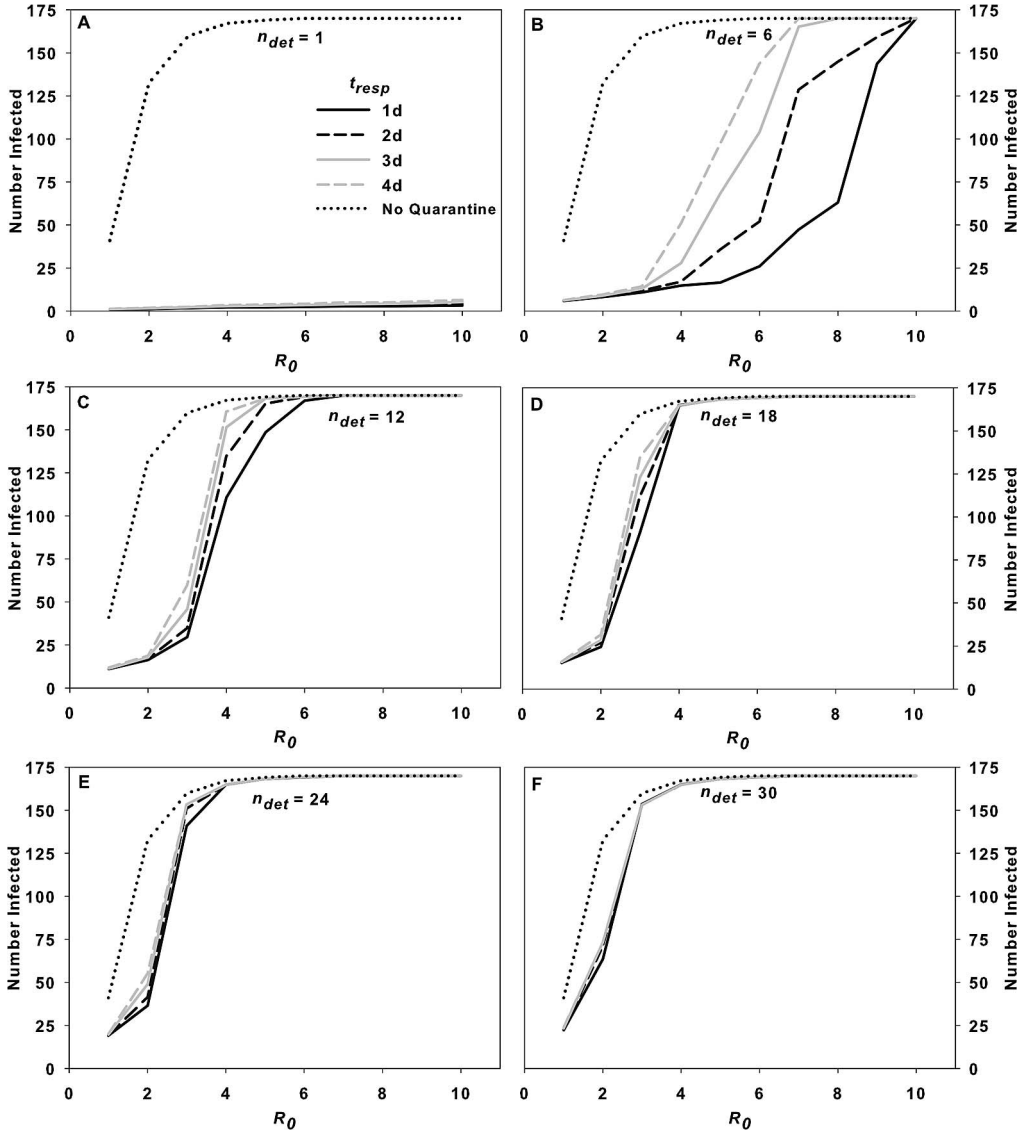
FIGURE 8.   Relationship between the mean number of Hawaiian monk seals (*Neomonachus schauinslandi*) infected during simulated morbillivirus outbreaks, the basic reproductive number (R_0), the threshold number of infectious seals for an outbreak to be detected (n_{det}), and the time from detection until quarantine is initiated (t_{resp}). For each of 1,000 baseline outbreak simulations, 1,000 quarantine scenarios were run. Panels A–F present increasing values of n_{det} (1, 6, 12, 18, 24, and 30) and values of t_{resp} from 1 to 4 d. In each panel the dotted line indicates the mean infected for baseline no-quarantine scenarios.

objective was achieved as evidenced by the correspondence of the mode of the simulated R_0 distribution with estimates of this parameter during actual epizootics in harbor seals (Fig. 3). This is reassuring, considering that the parameter space for contact rate and duration of the infectious period (the variables used to calculate R_0 since population size was fixed) was derived from behavioral observations of Hawaiian monk seals and studies of captive harbor seals infected with PDV, respectively. The baseline scenarios also support apprehension regarding morbillivirus in monk seals, as 91% of the simulated

outbreaks in a randomly mixing population of 170 seals had $R_0 > 1$, and in a third of cases nearly the entirely population was infected.

Heterogeneous contact patterns can profoundly influence the trajectory of disease outbreaks (Bansal et al. 2007), yet the statistically significant differences in contact rates estimated among Hawaiian monk seal size and sex classes (Baker et al. 2016a) had no appreciable effect on simulated outbreak results (Fig. 5). This allowed us to assume confidently homogeneous contact in the vaccination, quarantine, and spatially structured scenarios, which greatly simplified model structure.

Perhaps the most practical result of this study was the determination that vaccination efforts in response to an outbreak cannot be relied upon to reduce the number of individuals infected effectively (Fig. 4). The crux of the failure of this approach is the prolonged period between vaccination and acquired immunity, which is not amenable to improvement without compromising vaccine safety. Prophylactic vaccination to achieve herd immunity prior to an outbreak appears to be the only viable vaccination strategy to protect monk seals against potential morbillivirus outbreaks. Although this requires immunizing a large proportion of the population, the small number of monk seals remaining and their accessibility makes this a feasible prevention strategy. Accordingly, a pilot prophylactic seal vaccination program was initiated in Hawaii in 2016 (Malakoff 2016).

The spatially structured SEIR simulation indicates that outbreaks in the main Hawaiian Islands monk seal population would be far less severe than they would be in a single, randomly mixing population of equal abundance. The low rate of movement among islands relative to the plausible ranges of latency and infectious period effectively limit contact and disease spread, so that ≤ 10 seals were infected in over 60% of the modelled scenarios (Fig. 6). Another benefit of the spatial structure of the main Hawaiian Islands is that it substantially reduces the number of seals that require vaccination to achieve herd immunity.

Despite the promise that prophylactic vaccination could shield Hawaiian monk seals against a morbillivirus outbreak, there are considerable uncertainties regarding whether available vaccines (developed for CDV) would in fact confer immunity to whatever strain of PDV might appear in these seals. Controlled studies of captive harbor seals indicate that commercially available recombinant vaccines for domestic species can be safely used in phocids and that vaccinated seals mount CDV antibody titers consistent with immunity (Quinley et al. 2013). Similar unpublished studies have been conducted in captive Hawaiian monk seals. However, actually challenging vaccinated individuals with viral infection in these studies was precluded.

Fortunately, our simulations suggest that quarantine could be an effective complementary or back up (should prophylactic vaccination fail) strategy. Quarantining even a relatively small number of infected seals has the potential to extinguish even severe (high R_0) outbreaks (Fig. 8A). However, the efficacy of quarantine is highly sensitive to outbreak detection and response times. These can be minimized by surveillance (including clinical monitoring, serology, histology, and PCR), planning, and preparedness. In conclusion, modeling indicates prophylactic vaccination and quarantine supported by vigilant surveillance are the best tools for mitigation of morbillivirus risks to endangered Hawaiian monk seals.

SUPPLEMENTARY MATERIAL

Supplementary material for this article is online at http://dx.doi.org/10.7589/2016-10-238R.

LITERATURE CITED

Aguirre AA, Keefe TJ, Reif JS, Kashinsky L, Yochem PK, Saliki JT, Stott JL, Goldstein T, Dubey JP, Braun R, et al. 2007. Infectious disease monitoring of the endangered Hawaiian monk seal. *J Wildl Dis* 43:229–241.

Baker JD, Harting AL, Barbieri MM, Johanos TC, Robinson SJ, Littnan CL. 2016a. Estimating contact rates of Hawaiian monk seals (*Neomonachus schauinslandi*) using social network analysis. *J Wildl Dis* 52: 533–543.

Baker JD, Harting AL, Johanos TC, Littnan CL. 2016b. Estimating Hawaiian monk seal range-wide abundance and associated uncertainty. *Endang Species Res* 31:317–324.

Baker JD, Harting AL, Wurth TA, Johanos TC. 2011. Dramatic shifts in Hawaiian monk seal distribution predicted from divergent regional trends. *Mar Mammal Sci* 27:78–93.

Bansal S, Grenfell BT, Meyers LA. 2007. When individual behaviour matters: Homogeneous and network models in epidemiology. *J R Soc Interface* 4:879–891.

Duignan PJ, Van Bressem MF, Baker JD, Barbieri M, Colegrove KM, De Guise S, de Swart RL, Di Guardo G, Dobson A, Duprex WP, et al. 2014. Phocine distemper virus: Current knowledge and future directions. *Viruses* 6:5093–5134.

Gordon CH, Banyard AC, Hussein A, Laurenson MK, Malcolm JR, Marino J, Regassa F, Stewart AM, Fooks AR, Sillero-Zubiri C. 2015. Canine distemper in endangered Ethiopian wolves. *Emerging Infect Dis* 21:824–832.

Grachev MA, Kumarev VP, Mamaev LV, Zorin VL, Baranova LV, Denikina NN, Belikov SI, Petrov EA, Kolesnik VS, Kolesnik RS, et al. 1989. Distemper virus in Baikal seals. *Nature* 338:209.

Heide-Jorgensen MP, Harkonen T. 1992. Epizootiology of the seal disease in the eastern North Sea. *J Appl Ecol* 29:99–107.

Jensen T, van de Bildt M, Dietz HH, Andersen TH, Hammer AS, Kuiken T, Osterhaus A. 2002. Another phocine distemper outbreak in Europe. *Science* 297: 209.

Johanos, T. C. 2015a. *Hawaiian Monk Seal Research Program Hawaiian monk seal master identification records (annual) collected at Laysan Island in 1991 and in the main Hawaiian Islands in 2014.* US National Oceanographic Data Center. https://inport.nmfs.noaa.gov/inport/item/12939. Accessed October 2015.

Johanos, TC 2015b. *Hawaiian Monk Seal Research Program Hawaiian monk seal master identification records (seal) collected at Laysan Island in 1991 and in the main Hawaiian Islands in 2014.* US National Oceanographic Data Center, https://inport.nmfs.noaa.gov/inport/item/5677. Accessed October 2015.

Kennedy S, Kuiken T, Jepson PD, Deaville R, Forsyth M, Barrett T, van de Bildt MWG, Osterhaus ADME, Eybatov T, Duck C, et al. 2000. Mass die-off of Caspian seals caused by canine distemper virus. *Emerging Infect Dis* 6:637–639.

Lonergan M, Hall A, Thompson H, Thompson PM, Pomeroy P, Harwood J. 2010. Comparison of the 1988 and 2002 phocine distemper epizootics in British harbour seal *Phoca vitulina* populations. *Dis Aquat Org* 88:183–188.

MacPhee RDE, Greenwood AD. 2013. Infectious disease, endangerment, and extinction. *Int J Evol Biol* 2013: 571939.

Malakoff M. 2016. A race to vaccinate rare seals. *Science* 352:1265.

Quinley N, Mazet JAK, Rivera R, Schmitt TL, Dold C, McBain J, Fritsch V, Yochem PK. 2013. Serologic response of harbor seals (*Phoca vitulina*) to vaccination with a recombinant canine distemper vaccine. *J Wildl Dis* 49:579–586.

Robinson SJ. 2016. *Hawaiian Monk Seal Research Program Hawaiian monk seal cell phone tag data collected in the main Hawaiian Islands.* US National Oceanographic Data Center. https://inport.nmfs.noaa.gov/inport/item/28583. Accessed September 2014.

Scheel DM, Slater GJ, Kolokotronis SO, Potter CW, Rotstein DS, Tsangaras K, Greenwood AD, Helgen KM. 2014. Biogeography and taxonomy of extinct and endangered monk seals illuminated by ancient DNA and skull morphology. *ZooKeys* 409:1–33.

Schultz JK, Baker JD, Toonen RJ, Bowen BW. 2009. Extremely low genetic diversity in the endangered Hawaiian monk seal (*Monachus schauinslandi*). *J Hered* 100:25–33.

Vynnycky E, White R. 2010. *An introduction to infectious disease modelling.* Oxford University Press, Oxford, UK, 370 pp.

Wilson KC. 2015. *Integrating multiple technologies to understand the foraging behaviour and habitat use of monk seals in the main Hawaiian Islands.* PhD Dissertation, Department of Marine Science and Conservation, Duke University, 132 pp.